

# VIRTUAL MESON CLOUD OF THE NUCLEON AND INTRINSIC STRANGENESS AND CHARM

S. Paiva<sup>2\*</sup>, M. Nielsen<sup>1†</sup>, F.S. Navarra<sup>1‡</sup>, F.O. Durães<sup>1§</sup>, and L.L. Barz<sup>1\*\*</sup>

<sup>1</sup>*Instituto de Física, Universidade de São Paulo  
C.P. 66318, 05389-970 São Paulo, SP, Brazil*

<sup>2</sup>*Instituto de Física Teórica, UNESP  
Rua Pamplona 145, 01405-901 São Paulo, SP, Brazil*

## Abstract

We have applied the Meson Cloud Model (MCM) to calculate the charm and strange antiquark distribution in the nucleon. The resulting distribution, in the case of charm, is very similar to the intrinsic charm momentum distribution in the nucleon. This seems to corroborate the hypothesis that the intrinsic charm is in the cloud and, at the same time, explains why other calculations with the MCM involving strange quark distributions fail in reproducing the low  $x$  region data. From the intrinsic strange distribution in the nucleon we have extracted the strangeness radius of the nucleon, which is in agreement with other meson cloud calculations.

PACS numbers 14.20.Dh 12.40.-y 14.65.-q

Many years ago, it has been suggested by Sullivan [1] that some fraction of the nucleon's anti-quark sea distribution may be associated with non-perturbative processes like the pion

---

\*e-mail: samya@if.usp.br

†e-mail: mnielsen@if.usp.br

‡e-mail: navarra@if.usp.br

§e-mail: dunga@if.usp.br

\*\* e-mail: lbarz@if.usp.br

cloud of the nucleon. The generalization of this process to other mesons is depicted in figs. 1a and b, and was used in refs. [2,3] to calculate the strange and anti-strange sea quark distributions in the nucleon.

Recent analysis of deep inelastic neutrino-hadron scattering data [4] renewed the interest on the meson cloud picture of the nucleon. It is well known that, in this picture there is an asymmetry between sea quark and anti-quark momentum distributions [2]. This happens because the quark and the anti-quark are in different hadronic bound states. On the other hand, in extracting sea distributions from hard processes, it is usually assumed that the quark and antiquark sea contributions are equal. From the point of view of QCD, no definite statement on this subject can be made. Based on charge conjugation symmetry it is only possible to say that the quark sea distribution in the nucleon is equal to the antiquark sea distribution in the antinucleon. In ref. [4] it is shown that, in contrast to the meson cloud approach expectation, the sea strange and anti-strange quark distributions are quite similar. At first sight this would be a very strong argument against the relevance of the meson cloud [5]. The attempt to explain experimental data with the meson cloud model performed in refs. [2,3] has shown not only that the asymmetry present in this model seems to be in conflict with data but also that the calculated distributions are far below data for  $x < 0.3$ . However, in ref. [6], these data were reconsidered and combined with the CTEQ collaboration analysis [7]. The conclusion of the authors was that, considering the error bars, existing data do not exclude some asymmetry between the strange and anti-strange momentum distributions, which is significant only for  $x > 0.2 - 0.3$ .

In the present work we apply the meson cloud model (MCM) to study strangeness and charm in the nucleon. In the case of strangeness, we shall try to extract some estimates on the strangeness radius of the nucleon. This is a very interesting quantity from both theoretical and phenomenological point of view. Indeed, approved parity-violating lepton scattering experiments at MIT-Bates [8] and CEBAF [9] will provide information on the strangeness form factors at low and intermediate  $Q^2$  values, and more precisely determine the strange radius and anomalous magnetic moment of the nucleon. In the anticipation of the forthcoming data, considerable discussion about the strange matrix elements of the nucleon, based primarily in nucleon models, have appeared in the literature. These nucleon model estimates [10–18] contain large theoretical uncertainties and their results may greatly differ from each other. For the strangeness (Sachs) radius, for instance, the predictions vary by over an order of magnitude and in their sign. A comparison of some of these estimates can be found in ref. [14].

We start drawing special attention to one point which, we believe, was not enough stressed in ref. [3,6], namely that there are two kinds of  $q\bar{q}$  fluctuations contributing to the nucleon wave function: intrinsic and extrinsic. We shall emphasize, in particular, that we can identify the distribution of the valence anti-quark in the meson cloud with the distribution of the corresponding intrinsic anti-quark [19]. Therefore, in order to fit data, one has necessarily to include the contribution of the extrinsic anti-quarks.

In order to show the close relation between the meson cloud and the intrinsic states we start in the charm sector where, due to large charm quark mass, there is a striking difference between intrinsic and extrinsic quark distributions. This makes interesting the application of the MCM to charm. Whereas the case of strangeness we can confront MCM predictions directly with data, in the case of charm we may confront a part of the MCM with the

intrinsic charm hypothesis (the eventual existence of accurate data on charm and anticharm distributions in the nucleon would allow us to test once more the MCM).

We shall calculate the intrinsic nucleon  $\bar{c}$  distribution,  $\bar{c}_N^{(i)}(x)$ , which, in the meson cloud approach is the convolution of the valence  $\bar{c}$  momentum distribution in the  $\bar{D}$  meson,  $\bar{c}_D^{(v)}(x)$ , with the momentum distribution of this meson in the nucleon  $f_D(y)$  :

$$x\bar{c}_N^{(i)}(x) = \int_x^1 dy f_D(y) \frac{x}{y} \bar{c}_D^{(v)}\left(\frac{x}{y}\right). \quad (1)$$

The virtual  $\bar{D}$  meson distribution in the nucleon's cloud which characterizes its probability of carrying a fraction  $y$  of the nucleon's momentum in the infinite momentum frame is given by [1]

$$f_D(y) = \frac{g_{DNA}^2}{16\pi^2} y \int_{-\infty}^{t_{max}} dt \frac{[-t + (m_\Lambda - m_N)^2]}{[t - m_D^2]^2} F^2(t), \quad (2)$$

where  $t = k^2$  is the meson virtuality. In the above equation  $F(t)$  is a form-factor at the  $DNA$  vertex, and  $t_{max}$  is the maximum value of  $k^2$ , determined purely by kinematics:

$$t_{max} = m_N^2 y - \frac{m_\Lambda^2 y}{1 - y}. \quad (3)$$

For the  $DNA$  form factor, following a phenomenological approach, we use the monopole form:

$$F(t) = \frac{\Lambda^2 - m_D^2}{\Lambda^2 - t}, \quad (4)$$

where  $m_N$ ,  $m_\Lambda$  and  $m_D$  are the nucleon mass, the mass of the intermediate  $\Lambda_c$  and the  $\bar{D}$  meson mass respectively.  $\Lambda$  is the form factor cut-off parameter. With this parametrization we can directly compare the results obtained here with those quoted in ref. [20].

In the heavy quark effective theory [21] it is assumed that the heavy quark interacting with light constituents, inside a hadronic bound state, exchanges momenta much smaller than its mass. Therefore, to a good approximation, the heavy quark moves with the velocity of the charmed hadron. Being almost on-shell, the heavy quark carries almost the whole momentum of the hadron. These considerations suggest that the  $\bar{c}$  distribution in the  $\bar{D}$  meson is expected to be quite hard. We shall start assuming that it is a delta function:

$$\bar{c}_D^{(v)}\left(\frac{x}{y}\right) \simeq \delta\left(\frac{x}{y} - 1\right) = x \delta(x - y). \quad (5)$$

Evaluating (1) with the previously [20] used values of  $g_{DNA} = -3.795$  and  $\Lambda = 1.2$  GeV we obtain for  $\bar{c}_N^{(i)}(x)$  the solid curve shown in figure 2. For comparison we show with a dashed line the intrinsic anti-charm distribution obtained by Brodsky [19]:

$$\bar{c}_N^{(i)}(x) = Nx^2 \left[ \frac{1}{3}(1-x)(1+10x+x^2) - 2x(1+x) \ln \frac{1}{x} \right], \quad (6)$$

where  $N$  is the same normalization constant used in [19]. As it can be seen, there is a striking similarity between both curves. Apart from details this result confirms our idea, that the

valence charm quarks in the cloud are intrinsic to the nucleon. It is also interesting to notice that with the parameters used above, the total area below the curve in fig. 2, which gives the total intrinsic charm of the nucleon, is  $\sim 0.02$ . This means that the two scenarios, the one described in ref. [20] which evaluate the intrinsic charm by relating it with the charm radius of the nucleon, and the one used here, which extract the intrinsic charm directly from the  $\bar{c}$  distribution of the nucleon, are consistent. They are also consistent with the intrinsic charm hypothesis of ref. [19].

In the strange sector, if we want the total  $\bar{s}$  distribution in the nucleon we have to consider not only the valence  $\bar{s}$  in the kaon, but also the sea  $\bar{s}$  quarks which are present in all hadronic intermediate states. Therefore, we have to consider processes in the type of fig. 1b, where the virtual photon strikes the recoiling baryon rather than the meson, in addition to the processes in fig. 1a. In ref. [2] only the valence  $s$  and  $\bar{s}$  quarks in the  $\Lambda$  and  $K$  intermediate states were considered when estimating respectively the  $s$  and  $\bar{s}$  distributions in the nucleon. As argued in the previous part of this letter, this gives only the intrinsic strangeness of the nucleon, and will fail to reproduce the total strange distribution of the nucleon at small  $x$  [2], where the extrinsic part is important. Also in ref. [2] it was assumed that the amplitude to find an intermediate baryon with momentum fraction  $y$  in the nucleon (process of fig.1b) is the same as to find an intermediate meson with momentum fraction  $(1 - y)$  in the nucleon (process of fig.1a). This assumption has enhanced the asymmetry between  $s$  and  $\bar{s}$  distributions in ref. [2]. The authors of ref. [22], on the other hand, have neglected the off-shellness of the recoiling baryon and have generated the baryon distribution in the nucleon's cloud. Also, an additional parameter was introduced to ensure that the model generates an equal amount of strangeness and antistrangeness and, therefore, no asymmetry was produced. In ref. [22] only valence quarks were considered in the intermediate states. In both works [2,22] one expected to determine the sea quark distribution in the nucleon from the knowledge only of the valence quark distributions of the various intermediate states.

In ref. [3] the authors did consider the sea  $\bar{s}$  (besides the valence  $\bar{s}$ ) distribution in the mesons, when calculating the  $\bar{s}$  distribution of the nucleon. However, they did not include the sea  $\bar{s}$  distribution in the intermediate baryons, and this cannot be justified. Of course the idea of considering the sea quarks in the intermediate baryons to evaluate the sea quark distribution in the nucleon leads to a self-consistent equation since one of the possible intermediate states is just the  $N\pi$  pair. Besides, one has also to know the sea  $\bar{s}$  distribution in  $\Delta$ ,  $\Lambda$ ,  $\Sigma$ ,  $\Sigma^*$  and all other intermediate baryons considered in the calculation, to extract the sea  $\bar{s}$  distribution in the nucleon. Since there is no experimental knowledge about all of them, it would be necessary to make further assumptions which would reduce (or maybe destroy) the predictive power of the MCM.

So far our preliminary conclusion is that the MCM has a simple version and may have a more complicated version. In the simple version (used in the past by many authors [2,22,23]) we identify the nucleon anti-quark content with the valence anti-quark in the meson cloud of the nucleon. This simple hypothesis has been shown to work well in the description of the large  $x$  ( $x > 0.3$ ) domain of the anti-strange distribution. The more elaborated version of the MCM should include the sea anti-quark component of the mesons and baryons. We believe that with a proper inclusion of the sea, the MCM would be able to account for the low  $x$  data as well. However, according to the discussion in the last paragraph, it is rather cumbersome to pursue this exercise, at least for the time being. Instead, we shall explore

the simple version of the MCM.

In the first part of this work, studying charm distributions in the nucleon, we have established the equivalence between the anti-quark distribution obtained in the simple MCM with the intrinsic anti-quark distribution. Now we make a further connection between the intrinsic strange content of the nucleon and the strange squared radius.

In ref. [20] it was suggested that the probability of observing the intrinsic Fock state  $|uudq\bar{q}\rangle$  is given by

$$P_{iq} = \frac{|r_q^2|}{|r_p^2|}, \quad (7)$$

where  $q = c, s$  or combined light flavors,  $r_p$  is the average barionic radius of the proton,  $r_p = [\langle r_p^2 \rangle]^{1/2} \simeq 0.72$  fm, and  $r_q^2$  is the average squared radius of the quark of flavor  $q$ .

The ratio between the average squared radii in the above formula has a simple geometrical interpretation. It gives us the relation between the typical size of the fluctuations of a certain flavor  $q$  and the “total size” of the nucleon, i.e., the size that takes into account all possible fluctuations that couple to isoscalar currents. Therefore, eq.(7) is a good measure of the probability that such fluctuation occurs. Since the intrinsic quark distribution functions in the nucleon give the probability to find the intrinsic quarks in the nucleon as a function of the fraction  $x$  of the nucleon’s momentum carried by the quark, we can use eq.(7) to extract the strangeness radius of the nucleon, by integrating its intrinsic strangeness distribution.

To evaluate the intrinsic strangeness of the nucleon we follow ref. [3] and include only the kaon as meson intermediate states, and the  $\Lambda$ ,  $\Sigma$  and  $\Sigma^*$  as hyperon intermediate states. Therefore, we can rewrite Eq.(1) as

$$x\bar{s}_N^{(i)}(x, Q^2) = \sum_Y \int_x^1 dy f_{KY}(y) \frac{x}{y} \bar{s}_K^{(v)}\left(\frac{x}{y}, Q^2\right). \quad (8)$$

Since we have included decuplet states as hyperon intermediate states, we need to generalize Eq.(2) to account for this possibility. Therefore, we write the kaon’s distribution in the nucleon’s cloud as

$$f_{KY}(y) = \tau_Y \frac{g_{KNY}^2}{16\pi^2} y \int_{-\infty}^{t_{max}} dt \frac{T(t, m_N, m_Y)}{[t - m_K^2]^2} F_{KNY}^2(t), \quad (9)$$

with

$$T(t, m_N, m_Y) = \begin{cases} -t + (m_Y - m_N)^2 & Y \in 8 \\ \frac{((m_Y + m_N)^2 - t)^2 ((m_Y - m_N)^2 - t)}{12m_N^2 m_Y^2} & Y \in 10 \end{cases}, \quad (10)$$

for an intermediate octet or decuplet hyperon. In the above equation  $t_{max}$  is still given by Eq.(3) only with  $m_\Lambda$  substituted by  $m_Y$ , the intermediate hyperon mass. In Eq.(9),  $\tau_Y$  is a spin-flavor SU(6) Clebsh-Gordon factor. For the kaon-hyperon couplings we follow ref. [3] and relate them to the pion-nucleon couplings using spin-flavor SU(6) [24]. The form factor,  $F_{KNY}(t)$ , at the nucleon-kaon-hyperon vertex is usually parametrized either in monopole, dipole or exponential form. To make a direct comparison with previous work easier, we will restrict ourselves to the exponential form:

$$F_{KNY}(t) = e^{(t-m_K^2)/\Lambda_{KNY}^2} , \quad (11)$$

with  $\Lambda_{KNY} = 1200$  MeV [3].

We neglect the small difference between the pion and kaon structure functions and use the better determined pion structure function to evaluate eq.(8). In figure 3 we present the  $\bar{s}_N^{(i)}$  distribution obtained with the help of the SMRS [25] parametrization of the pion structure function extracted from fits to Drell-Yan pair production experiments. From this figure we get  $P_{is} = 0.12$ . It is very interesting to notice that the authors of ref. [26], using the MIT bag model to calculate the probability of finding a five-quark component  $|uudq\bar{q}\rangle$  configuration bound within the nucleon bag, got  $P_{ic} = 0.02$  and  $P_{is} = 0.16$ , in good agreement with our results.

Comparing fig.3 with fig.2 we find that the intrinsic charm carries more momentum than the intrinsic strangeness, as expected. The shape of the intrinsic strangeness distribution seems very similar to the usual parametrizations of sea-quark distributions. However, as it can be seen in fig.4, it has a very important difference with respect to the real sea distribution:  $x\bar{s}_N^{in}(x)$  goes to zero as  $x$  goes to zero. In fig.4 we also show the CCFR data [4], and the  $\bar{s}$  distribution calculated in ref. [3] with the help of the GRV [27] parametrization for the pion structure function. From this figure we clearly see that for  $x > 0.3$  the intrinsic distribution can fairly well describe the data.

In fig.3 we also plot the individual contribution of each intermediate pair considered in our calculation. As can be seen, the contribution from the  $\Sigma - K$  pair is much smaller than the others, due to the smaller coupling constant. This was expected and this contribution was even neglected in refs. [11,12,14] due to this reason. However, the contribution of the  $\Sigma^* - K$  pair is of the same order of magnitude as the  $\Lambda - K$  pair and cannot be neglected. Using the value  $P_{is} = 0.12$  in the above relation, eq.(7), we get for the strangeness radius

$$| \langle r_s^2 \rangle | = 6.22 \times 10^{-2} fm^2 . \quad (12)$$

If we still add to it the vector-meson dominance model contribution coming from the  $\omega - \phi$  mixing [12] we get

$$| \langle r_s^2 \rangle | = 7.97 \times 10^{-2} fm^2 , \quad (13)$$

which is about two times the result in ref. [12] and only less than half of the result in ref. [10]. It is worth mentioning that we can not predict the sign of the square strangeness radius in our approach.

If we had considered only the  $\Lambda - K$  loop in our calculations, instead of  $\Lambda - K$ ,  $\Sigma - K$  and  $\Sigma^* - K$  as we did, we would have got  $P_{is} = 0.0585$ . This would reduce the strangeness radius to  $| \langle r_s^2 \rangle | = 3.03 \times 10^{-2} fm^2$ , which is completely consistent with the medium value obtained in ref. [11]:  $| \langle r_s^2 \rangle | = 2.5 \times 10^{-2} fm^2$ . This value was obtained by probing the  $\Lambda - K$  loop with a vector strange current.

To summarize, based in our results, we would like to stress that the strangeness radius of the nucleon will be experimentally accessible in the near future. From the theoretical point of view it is not yet clear how to calculate it precisely. Some of the theoretical works concentrate on the computation of the strange vector form factors from mesonic loops. So far a complete computation of all loops, including all the relevant hadrons, is not available.

Our estimates, based on the intrinsic strangeness of the nucleon, are useful guides, and give us the relative importance of each mesonic loop. In particular our calculation strongly indicates that the  $\Sigma^* - K$  loop should be included in form-factor computations [28].

Acknowledgements: This work has been supported by FAPESP and CNPq. We would like to warmly thank S.J. Brodsky and W. Koepf instructive discussions.

## REFERENCES

- [1] J.D. Sullivan, *Phys.Rev.* **D5**, 1732 (1972).
- [2] A.I. Signal and A.W. Thomas, *Phys. Lett.* **B191**, 205 (1987).
- [3] W. Koepf, L.L. Frankfurt and M. Strikman, *Phys.Rev.* **D53**, 2586 (1996).
- [4] CCFR Collaboration, A.O. Bazarko et al., *Z. Phys.* **C65**, 189 (1995).
- [5] X. Ji and J. Tang, *Phys. Lett.* **B362**, 182 (1995).
- [6] S.J. Brodsky and B.Q. Ma, SLAC report, SLAC-PUB-7126.
- [7] CTEQ Collab., J. Botts et al., *Phys. Lett.* **B304**, 159 (1993); W.L. Lai et al., *Phys.Rev.* **D51**, 4763 (1995).
- [8] MIT-Bates Proposal No. 89-06, R.D. McKeown and D.H. Beck, contact people.
- [9] CEBAF Proposal No. PR-91-004, E.J. Beise, spokesperson; CEBAF Proposal No. PR-91-010, J.M. Finn and P.A. Souder, spokespersons; CEBAF Proposal No. PR-91-017, D.H. Beck, spokesperson.
- [10] R. L. Jaffe, *Phys. Lett.* **B229**, 275 (1989).
- [11] M.J. Musolf and M. Burkardt, *Z. Phys.* **C61**, 433 (1994).
- [12] T.D. Cohen, H. Forkel and M. Nielsen, *Phys. Lett.* **B316**, 1 (1993).
- [13] S. Hong and B. Park, *Nucl. Phys.* **B561** 525 (1993).
- [14] H. Forkel, M. Nielsen, X. Jin and T.D. Cohen, *Phys.Rev.* **C50**, 3108 (1994).
- [15] W. Koepf and E.M. Henley, *Phys.Rev.* **C49**, 2219 (1994); W. Koepf, S.J. Pollock and E.M. Henley, *Phys. Lett.* **B288**, 11 (1992).
- [16] H.-W. Hammer, Ulf-G. Meißner and D. Drechsel, *Phys. Lett.* **B367**, 323 (1996).
- [17] H. Forkel, preprint hep-ph/951226; hep-ph/9607429.
- [18] M.J. Musolf and H. Ito, preprint nucl-th/9607021.
- [19] S.J. Brodsky, C. Peterson and N. Sakai, *Phys.Rev.* **D23**, 2745 (1981); S. J. Brodsky, P. Hoyer, C. Peterson and N. Sakai, *Phys. Lett.* **B93**, 451 (1980).
- [20] F.S. Navarra, M. Nielsen, C.A.A. Nunes and M. Teixeira, *Phys.Rev.* **D54**, 842 (1996).
- [21] M. Neubert, *Phys. Rep.* **245**, 259 (1994).
- [22] W.-Y.P. Hwang, J. Speth and G.E. Brown, *Z. Phys.* **A339**, 383 (1991).
- [23] S. Kumano, *Phys.Rev.* **D43**, 59 (1991).
- [24] B. Holzenkamp, K. Holinde and J. Speth, *Nucl. Phys.* **A500**, 485 (1989).
- [25] P.J. Sutton, A.D. Martin, R.G. Roberts and W.J. Stirling, *Phys.Rev.* **D45**, 2349 (1992).
- [26] J.F. Donoghue and E. Golowich, *Phys.Rev.* **D15**, 3421 (1977).
- [27] M. Glück, E. Reya and A. Vogt, *Z. Phys.* **C53**, 651 (1992).
- [28] H. Forkel, M.J. Musolf, F.S. Navarra, M. Nielsen, work in progress.



## Figure Captions

- Fig. 1** The generalized Sullivan process. a) the virtual photon strikes the cloud meson. b) the virtual photon strikes the recoiling baryon.
- Fig. 2**  $\bar{c}_N(x)$  distribution calculated with the meson cloud model (solid line) and the intrinsic anti-charm distribution (dashed line).
- Fig. 3** Intrinsic  $\bar{s}_N(x)$  distribution calculated with the meson cloud model using the NA10 pion structure function (solid line). The individual contributions are:  $\Lambda - K$  (dotted line),  $\Sigma - K$  (dot-dashed line) and  $\Sigma^* - K$  (dashed line).
- Fig. 4** Intrinsic  $x\bar{s}_N(x)$  distribution calculated with the meson cloud model using the NA10 pion structure function (solid line). The data are from the CCFR collaboration and the dashed line shows the calculation of ref.[3].

**Figure 1**

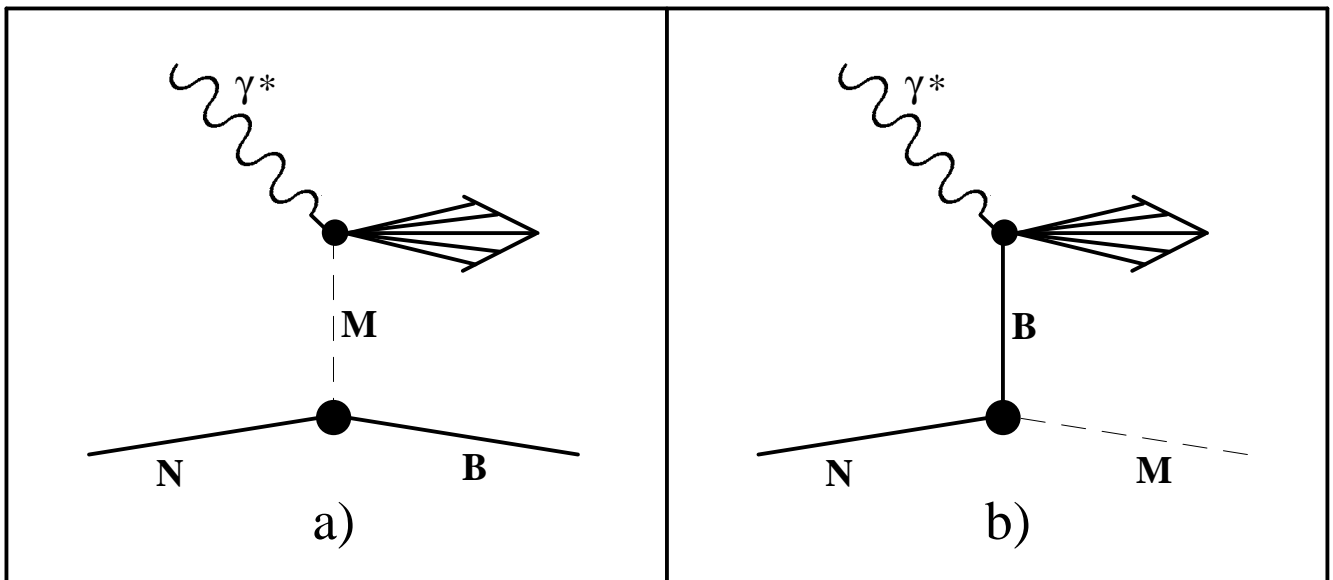


**Figure 2**

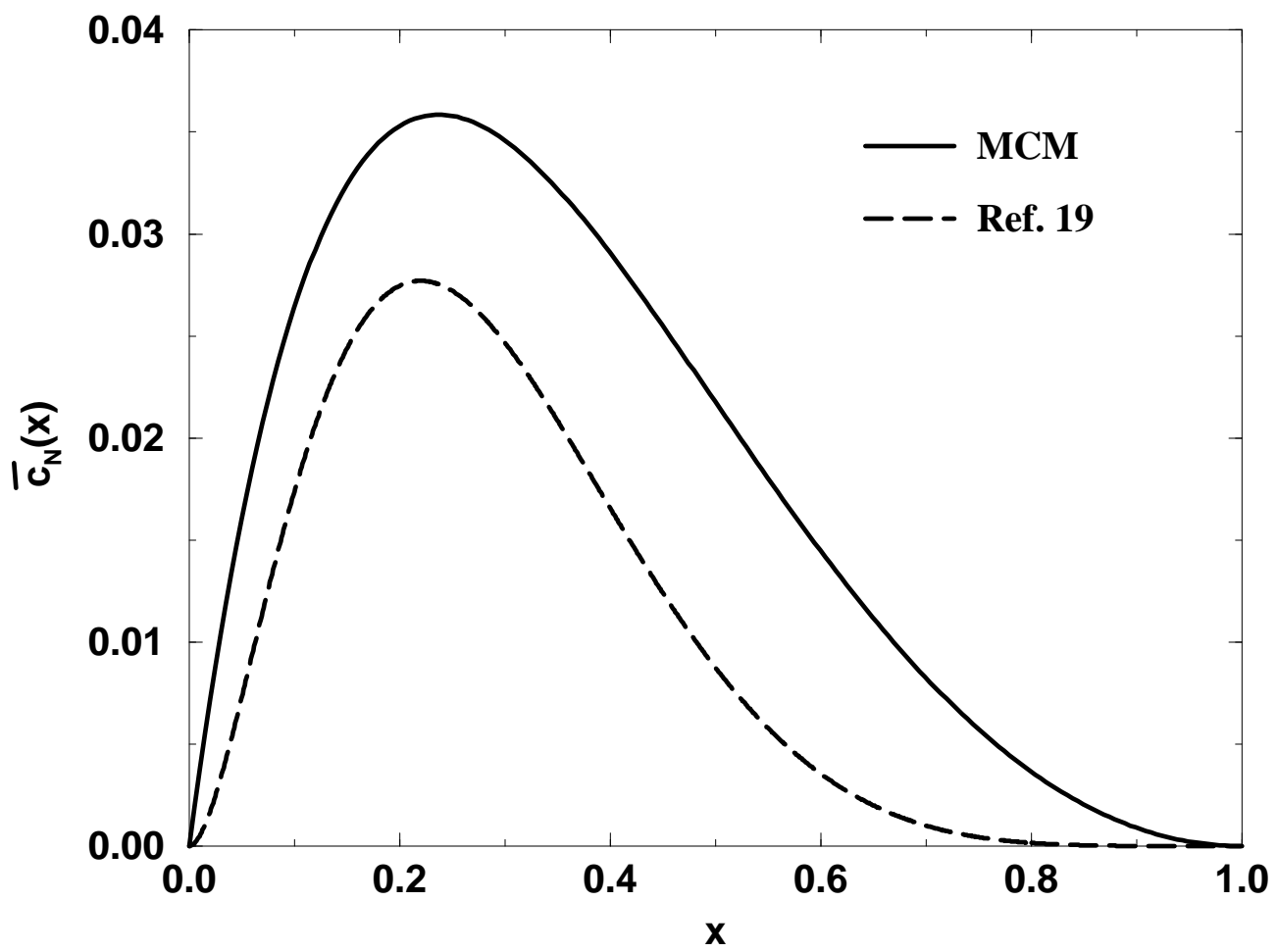


**Figure 3**

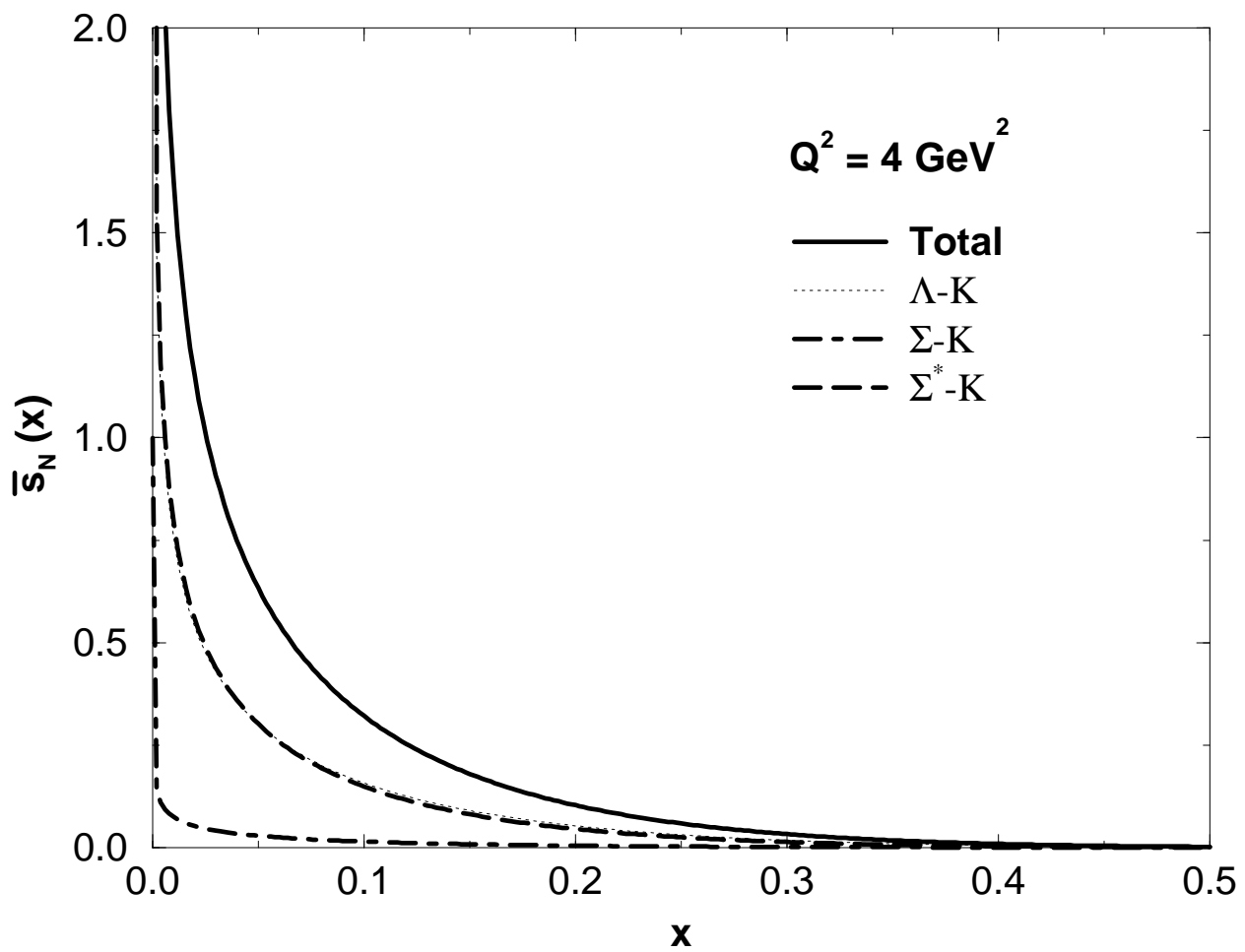


**Figure 4**

